Arabian Journal of Chemistry (2023) **16**, 104659

King Saud University

Arabian Journal of Chemistry

www.ksu.edu.sa
www.sciencedirect.com

ORIGINAL ARTICLE

Synthesis and anti-α-glucosidase activity evaluation of betulinic acid derivatives

Xiao-Zheng Wu [a], Wen-Jian Zhu [a,b], Li Lu [a], Chun-Mei Hu [a], Ying-Ying Zheng [a], Xin Zhang [a], Jing Lin [a], Jing-Ying Wu [a], Zhuang Xiong [a], Kun Zhang [a], Xue-Tao Xu [a,*]

[a] *School of Biotechnology and Health Sciences, Wuyi University, Jiangmen 529020, PR China*
[b] *State Key Laboratory of Natural Medicines and Department of Medicinal Chemistry, China Pharmaceutical University, Nanjing 210009, PR China*

Received 12 July 2022; accepted 6 February 2023
Available online 11 February 2023

KEYWORDS

Betulinic acid;
Synthesis;
a-Glucosidase inhibitor;
Docking

Abstract In this article, a series of betulinic acid derivatives (**3a** ∼ **3u**, **4a** ∼ **4e**) were synthesized through a stepwise structure optimization and evaluated for their anti-α-glucosidase activities. All synthesized derivatives exhibited stronger anti-α-glucosidase activities (IC_{50}: 0.56 ± 0.05 ∼ 3.99 ± 0.23 μM) than betulinic acid (IC_{50}: 7.21 ± 0.58 μM) and acarbose (IC_{50}: 611.45 ± 15.51 μM). Compound **3q** presented the outstanding inhibitory activity (IC_{50}: 0.56 ± 0.05 μM), which was ∼ 1100 time stronger than that of acarbose. Compound **3q** was revealed as a reversible and noncompetitive α-glucosidase inhibitor by inhibitory mechanism assay. Fluorescence spectra, 3D fluorescence and CD spectra results showed that the interaction of compound **3q** with α-glucosidase caused the conformational and secondary structure content change of α-glucosidase. Finally, the molecular docking simulated the interaction between compound **3q** with α-glucosidase and the physicochemical parameter was assessed using SwissADME software.

1. Introduction

Diabetes mellitus is one of chronic metabolic diseases, that requires long-term drug intervention to regulate blood sugar levels (DeFronzo et al., 2015; Kahn et al., 2014). Type 2 diabetes is predominant in diabetes, more than 90 % of all cases (Adeghate et al., 2006; Guariguata et al., 2014). The insufficient insulin secretion and insulin resistance leads to hyperglycemia, that is the hallmark of diabetes (Wang et al., 2020). Thence, glucose control is a key strategy to treat diabetes (Deng et al., 2022). Inhibiting hydrolase enzymes of carbohydrate such as α-glucosidase can obviously control the postprandial hyperglycemia and reduce the risk of diabetes complications (Rafique et al., 2020; Zheng et al., 2021).

α-Glucosidase is an important enzyme in the small intestine, that can catalytic hydrolysis the carbohydrates to produce

* Corresponding author.
E-mail address: xuetaoxu@wyu.edu.cn (X.-T. Xu).
Peer review under responsibility of King Saud University.

Production and hosting by Elsevier

https://doi.org/10.1016/j.arabjc.2023.104659
1878-5352

glucose (Dhameja and Gupta, 2019; Ghani, 2015). α-Glucosidase inhibitors can block the activity of α-glucosidase, resulting in the regulation of the blood glucose and postprandial hyperglycemia (Ali et al., 2017; Hameed et al., 2019). Up to now, only several α-glucosidase inhibitors including voglibose, acarbose, and miglitol have been used clinically to treat type-2 diabetes (Wang et al., 2018; Wang et al., 2017; Wang et al., 2017). However, their long-term use leads to some side effects such as flatulence and diarrhea. Therefore, to find efficient and safer α-glucosidase inhibitors has attracted more and more attention.

Betulinic acid (BA, Fig. 1) is a natural pentacyclic lupane-type triterpenoid, mainly isolated from birch bark (Zhang et al., 2017). In recent years, scientific researches have revealed that BA is a very valuable natural star compound. BA and its derivatives have shown an array of pharmacological activities, including anti-cancer, anti-viral, and anti-inflammatory (Catteau et al., 2018; Kim et al., 2014; Putta et al., 2016). Moreover, BA shows effective antidiabetic effects due to its inhibition activity against α-glucosidase (IC_{50} = 10.6 μM) and human PTP1B (IC_{50} = 3.5 μM) (Ding et al., 2018; Ramirez-Espinosa et al., 2011). Besides, some BA derivatives have been reported as potential α-glucosidase agents, such as 2,3-indolobetulinic acid derivatives (Khusnutdinova et al., 2019), methyl ester derivatives of betulinic acid (Khusnutdinova et al., 2017), amide derivatives of betulinic acid (Kazakova et al., 2020), and *N*-allylated/*N*-alkylated niacin hybrids derivatives of betulinic acid (Narender et al., 2013) (Fig. 1). Also, combining with our research results on the structural modification of triterpenoid, including oleanolic acid and ursolic acid, we believe that structural modification of BA would be an effective strategy to develop novel α-glucosidase inhibitors.

On the other hand, styrene group is an important substituent in many pharmacologically compounds, such as chalcone derivatives (Leong et al., 2018); coumarin derivatives (Saeedi et al., 2017; Zawawi et al., 2015); cinnamic acid derivatives (Xu et al., 2020). Most of them present hypoglycemic and anti-α-glucosidase activity. For developing BA derivatives as potential α-glucosidase inhibitors, bioactive substituent of styrene was incorporated into BA skeleton *via* the hybridization strategy. In addition, synthesized BA derivatives were assayed for their α-glucosidase.

2. Results and discussion

2.1. Chemistry

The BA derivatives **3a** ~ **3u** were firstly synthesized using BA as starting material (Schemes 1). BA (**1**) was oxidized to produce betulonic acid **2** under 2-Iodoxybenzoic acid (IBX). Betulonic acid **2** underwent Claisen-Schmidt condensation reaction with substituted aldehydes to yield BA derivatives **3a** ~ **3u**.

The BA derivatives **4a** ~ **4e** were subsequently synthesized using **3q** as starting material (Schemes 2). All synthesized BA derivatives were identified by ^{1}H NMR, ^{13}C NMR and HRMS.

2.2. α-Glucosidase inhibitory activity assay and SAR study

The α-glucosidase inhibitory activities of BA derivatives **3a** ~ **3u** were firstly assayed and the results were listed in Table 1. The results revealed that BA derivatives **3a** ~ **3u** presented potent inhibitory activity toward α-glucosidase (IC_{50} from 0.56 ± 0.05 μM to 3.99 ± 0.23 μM), which was stronger than BA (IC_{50}: 7.21 ± 0.58 μM) and standard control acarbose (IC_{50} 611.45 ± 15.51 μM, $P < 0.05$). The results showed that the incorporation of styrene at **C-28** position of BA could effectively strengthen its α-glucosidase inhibitory activity.

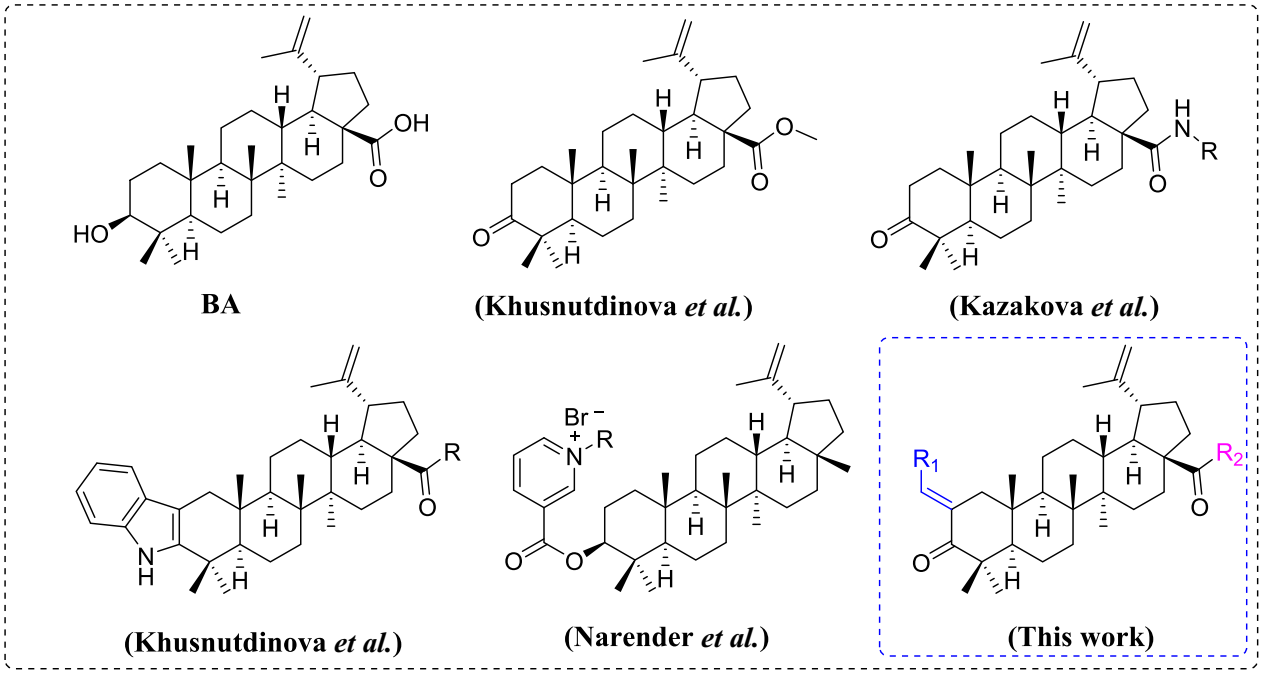

Fig. 1 Chemical structures of some reported α-glucosidase inhibitors.

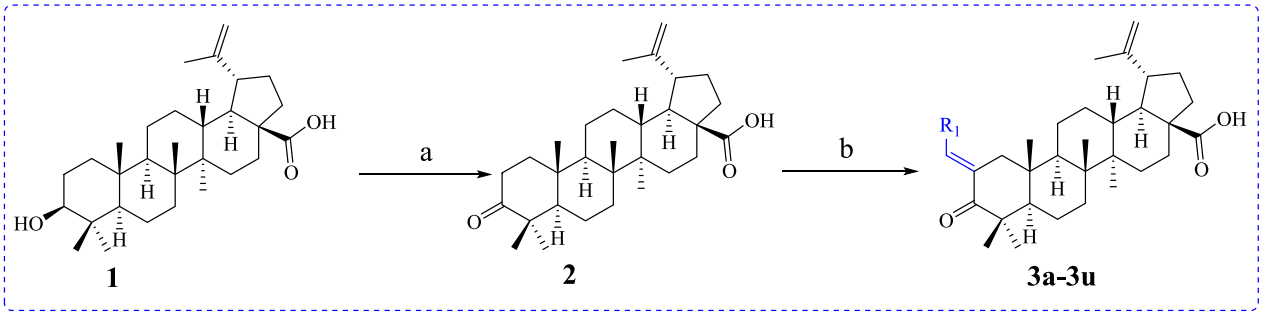

Scheme 1 Synthesis of BA derivatives **3a** ~ **3u**. Reagents and condition: (a) IBX, DMSO, 0 °C; (b) NaOH, EtOH, rt.

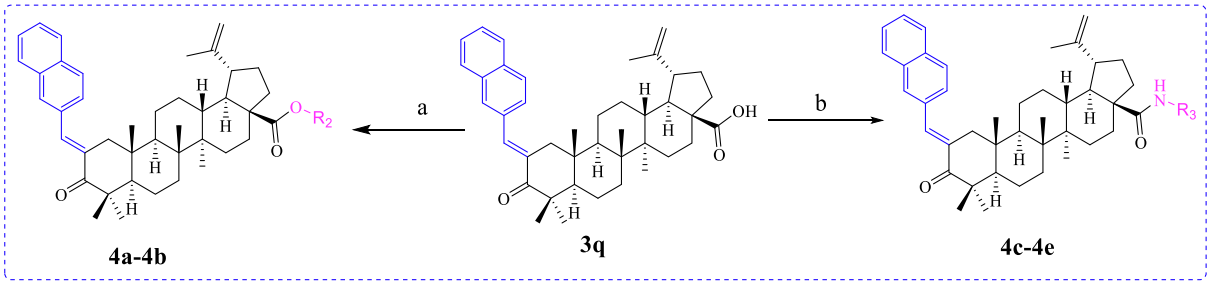

Scheme 2 Synthesis of BA derivatives **4a** ~ **4e**. Reagents and condition: (a) CH_3I or benzyl bromide, K_2CO_3, DMF, rt; (b) HATU, DIPEA, DMF, 0 °C.

Among them, derivative **3q** showed the strogest inhibitory activity (IC_{50}: 0.56 ± 0.05 μM). Thence, the structural modification of BA might be a benefit method for improving its anti-α-glucosidase activity and obtaining potential inhibitors.

For revealing the effect of different substituents on anti-α-glucosidase inhibitory, structure–activity relationship (SAR) was analyzed using derivative **3a** as template compound that had no substituent at benzene ring. For BA derivatives **3b** ~ **3q** with different substituent at benzene ring, BA derivatives **3b** ~ **3o** presented lower inhibitory activities than derivative **3a**, suggesting the introduction of CH_3, $C(CH_3)_3$, OCH_3, F, Cl, CF_3, NO_2, CN, C_6H_5, $N(CH_3)_2$, SO_2CH_3, $(OCH_3)_2$, $(OCH_3)_3$, or N_3H_2 reduced the inhibitory activity. While, BA derivatives **3p** (phenyl ether) and **3q** (naphthalene) showed stronger inhibitory activities than derivative **3a**, indicating that the introduction of phenyl ether or naphthalene enhanced the inhibitory activity. The results showed that the substituents at benzene ring might not be benefit for their anti-α-glucosidase inhibitory, except substituents with conjugate properties, such as phenyl ether and naphthalene. Moreover, the introduction of heterocycle (thiophene (**3r**), furan (**3s**), pyridine (**3t**)) and naphthenic (cyclohexane (**3u**)) pulled the inhibitory activity lower, compared to derivative **3a**. The results indicated that the heterocycle was adverse compared to benzene ring.

In order to obtain more potent inhibitors, the carboxyl moiety of BA was optimized based on compound **3q** with naphthalene group, yielding BA derivatives **4a** ~ **4e**. Unfortunately, their inhibitory activity assay results showed that the introduction of ester group, amino group, or piperazine group reduced their α-glucosidase inhibitory activities. The results indicated that the carboxyl moiety was critical for keeping the anti-α-glucosidase activity of BA comparing to ester and amide group. All above results gave useful guidance information for the structural modification of BA.

2.3. Inhibitory mechanism assay

Compound **3q** (IC_{50}: 0.56 ± 0.05) with strongest inhibitory activity was selected as representative compound to assay their inhibitory mechanism. Fig. 2a showed the plots of initial velocity of the enzymatic reaction *via* α-glucosidase concentration in the absence and presence of compound **3q** at different concentrations. The plots were straight lines with different positive slopes and passed through the ordinate origin, implied that compound **3q** inhibited α-glucosidase activity through the reversible inhibition mode (Yang et al., 2021).

The inhibition type of α-glucosidase by compound **3q** was assayed by Lineweaver-Burk plots (Fig. 2b). The slope of plot increased with the increase of compound **3q** concentration, and all lines intersected at one point on the × axis. These results were coinciding with the traits of noncompetitive inhibition (Yang et al., 2021). In addition, the slops *via* compound **3q** concentrations to give the inhibition constant (K_I) was calculated as 0.295 μM.

2.4. Fluorescence quenching analysis

To understand the inhibitory mechanism of compound **3q** against α-glucosidase, the effect of compound **3q** on the fluorescence of α-glucosidase was analyzed. It could be seen that α-glucosidase appeared an emission peak at 340 nm, which was decreased by the addition of compound **3q** (Fig. 3a ~ d). The results revealed that compound **3q** could

Table 1 The α-glucosidase inhibitory activity of all synthesized BA derivatives.

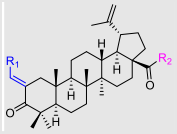

Compound	R_1	R_2	IC_{50} (μM)
3a		OH	1.06 ± 0.07[a]
3b		OH	2.63 ± 0.09[a]
3c	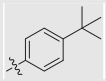	OH	1.11 ± 0.05[a]
3d		OH	2.91 ± 0.34[a]
3e		OH	3.06 ± 0.26[a]
3f	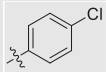	OH	1.89 ± 0.08[a]
3g	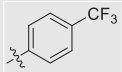	OH	1.39 ± 0.06[a]
3h	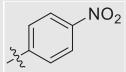	OH	2.58 ± 0.15[a]
3i	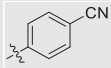	OH	1.90 ± 0.06[a]
3j	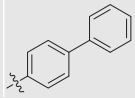	OH	1.40 ± 0.03[a]
3k	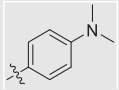	OH	3.43 ± 0.23[a]
3L	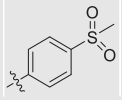	OH	2.10 ± 0.19[a]
3m	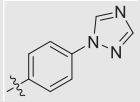	OH	2.23 ± 0.17[a]
3n	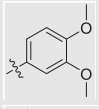	OH	3.69 ± 0.33[a]
3o	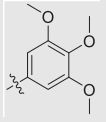	OH	3.25 ± 0.21[a]
3p	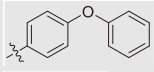	OH	0.86 ± 0.06[a]
3q	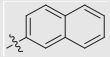	OH	0.56 ± 0.05[a]
3r		OH	1.67 ± 0.05[a]

Table 1 (*continued*)

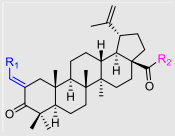

Compound	R_1	R_2	IC_{50} (μM)
3s		OH	2.03 ± 0.07[a]
3t		OH	2.12 ± 0.16[a]
3u		OH	1.37 ± 0.11[a]
4a	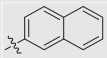		3.39 ± 0.28[a]
4b	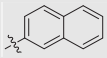	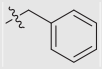	2.71 ± 0.17[a]
4c	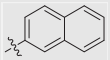	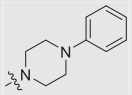	3.98 ± 0.22[a]
4d	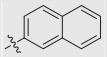		3.92 ± 0.15[a]
4e	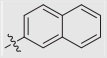	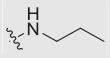	3.99 ± 0.23[a]
BA			7.21 ± 0.58[a]
Acarbose			611.45 ± 15.51

The standard error was obtained from four replicates. [a]$P < 0.05$, compared to acarbose.

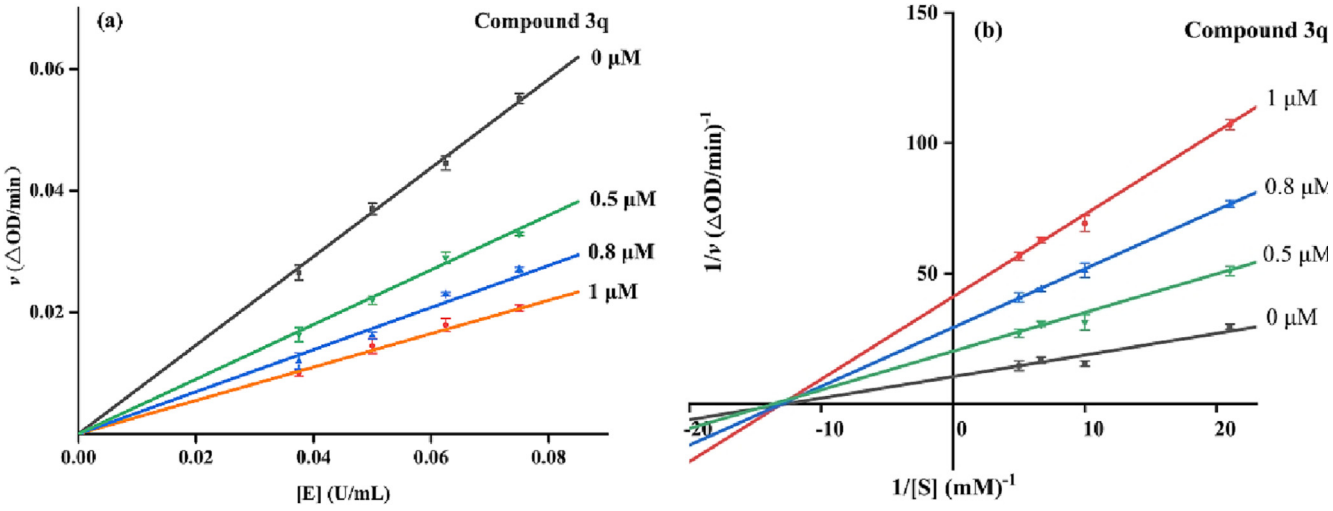

Fig. 2 (a) The initial velocity *via* α-glucosidase concentration in the absence and presence of compound **3q**; (b) Lineweaver-Burk plots for the inhibition α-glucosidase in the absence and presence of compound **3q**.

interact with α-glucosidase, leading to the conformation change of α-glucosidase. Also, the fluorescence quenching degree of α-glucosidase by compound **3q** was slightly increased with the increase of temperature.

The quenching mechanism was analyzed by Stern Volmer equation and the results (Table 2) showed that the quenching constant (Ksv) was increased with the increase of temperature, revealing a static quenching. The binding

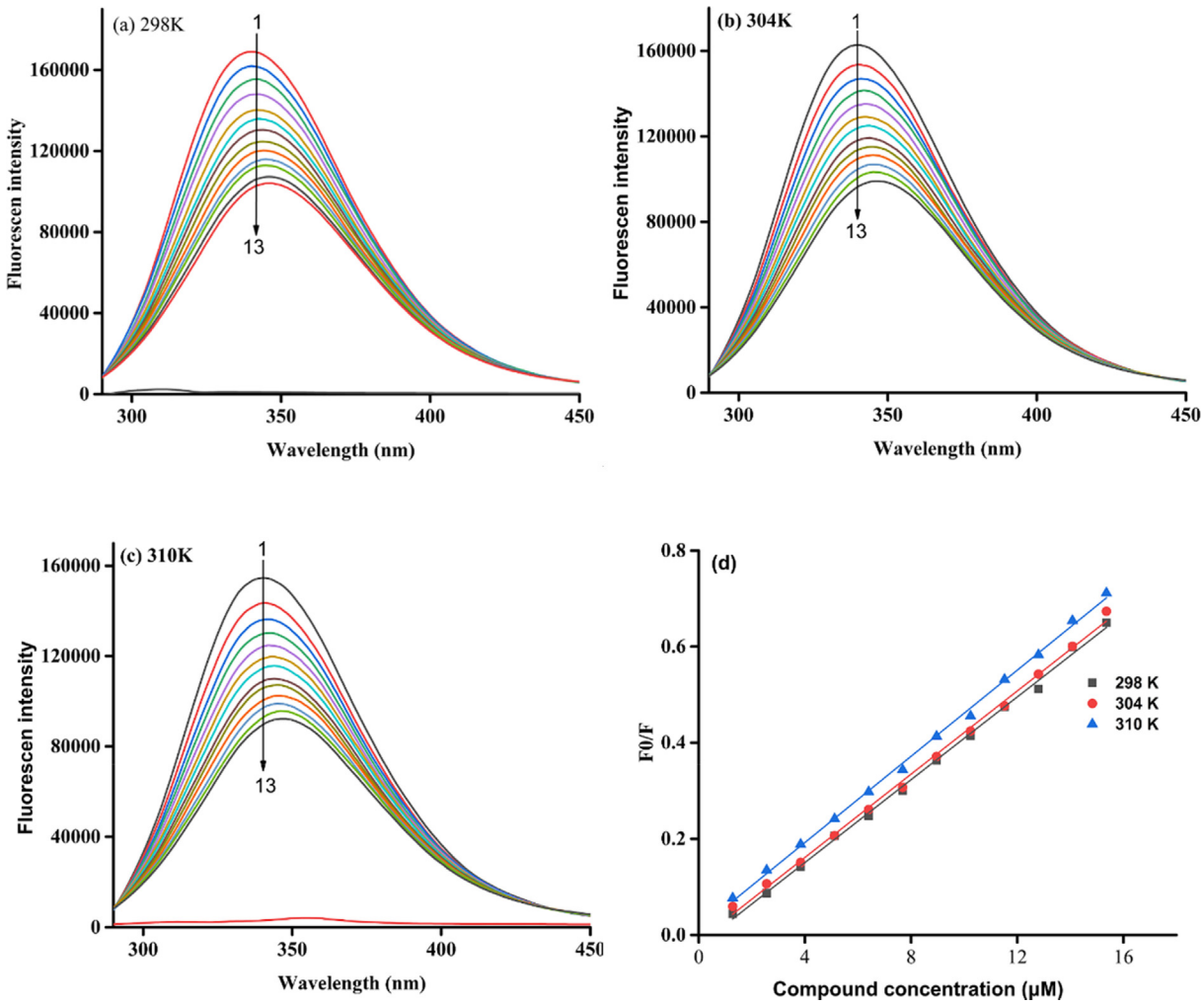

Fig. 3 Fluorescence spectra of α-glucosidase in the presence of compound **3q**. (a) 289 K, (b) 304 K, (c) 310 K. Compound **3q** concentration of curves 1–13 were 0, 1.28, 2.56, 3.84, 5.12, 6.4, 7.68, 8.96, 10.24, 11.52, 12.8, 14.08, and 15.36 μM respectively, (d) the Stern-Volmer plots of α-glucosidase quenched by compound **3q**.

Table 2 The quenching parameters of compound **3q** interacting with α-glucosidase.

T(K)	K_{SV} ($\times 10^5$ L mol^{-1})	Ka ($\times 10^5$ L mol^{-1})	n	△H (KJ/moL)	△G (KJ/moL)	△S (J/(mol·K)
298	4.31	1.59	1.09	−78.17	−29.67	−147.67
304	4.33	6.80	0.99		−33.28	
310	4.48	8.24	0.90		−33.75	

constants were greater than 10^5 L mol^{-1}, and the binding bits number was approximately equal to 1. At the same time, the thermodynamic parameters were calculated using the Van't Hoff and the Gibbs-Helmholtz Eq. The negative values of ΔG suggested the forming of complexes occurring spontaneously, and negative values of ΔH and ΔS implied the mainly interaction being hydrogen band and van der Waals forces.

2.5. 3D fluorescence spectra assay

3D fluorescence spectra assay was carried out to analyze the effect of compound **3q** toward the conformational change of α-glucosidase. As shown in the 3D fluorescence spectra of α-glucosidase (Fig. 4a), Tyr with Trp residues appeared spectral properties at peak **1** (λex = 280 nm, λem = 340 nm), protein structure transition from the n → π* caused the fluorescence

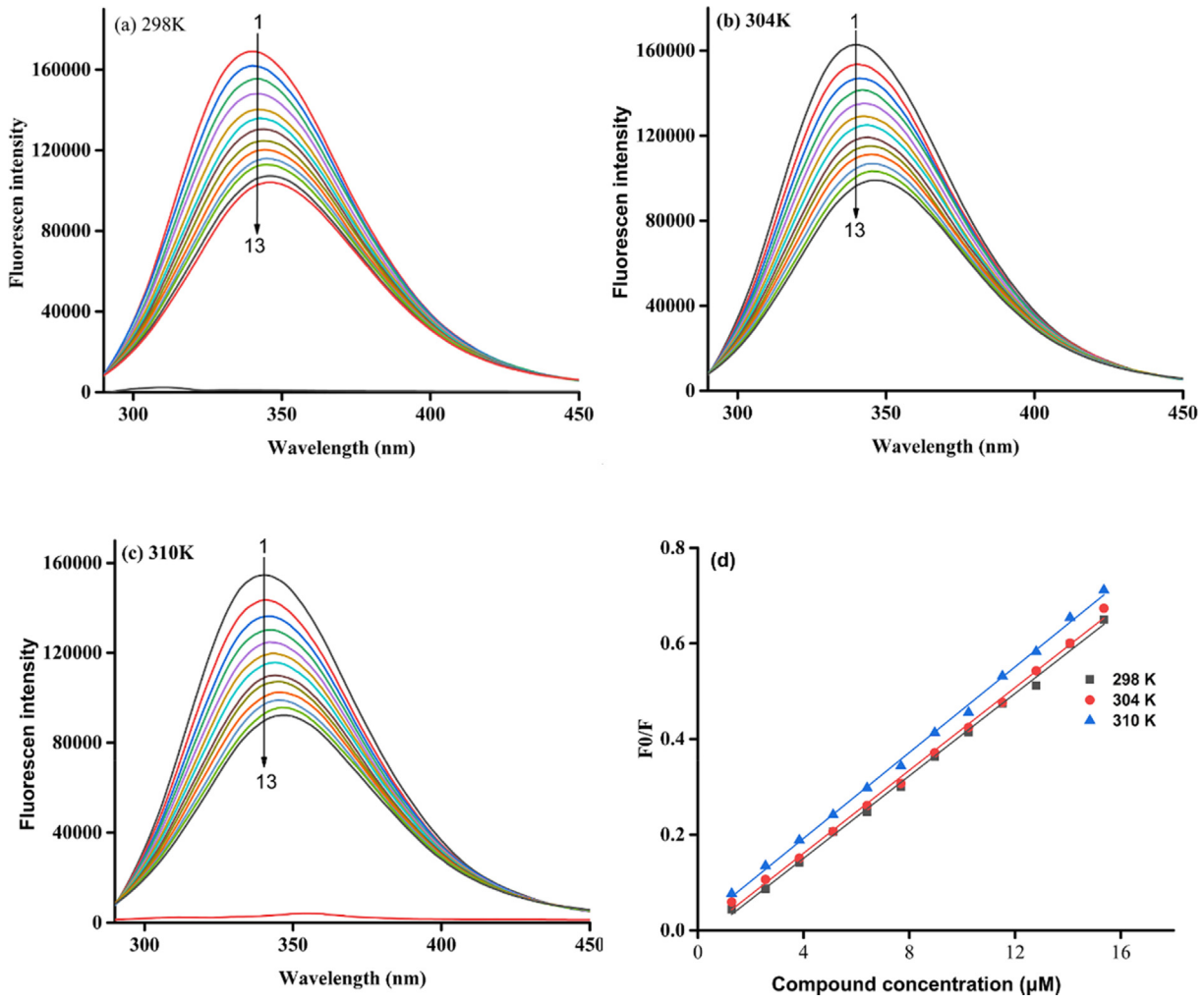

Fig. 4 The 3D fluorescence spectra of α-glucosidase (a) and α-glucosidase with compound **3q** system (b).

feature at peak **2** (λex = 225 nm, λem = 340 nm). However, the fluorescence intensity of peak **1** reduced by 11.93 %, and Peak **2** reduced by 34.64 %, after treated with compound **3q** (Fig. 4b). The results showed that the interaction of compound **3q** with α-glucosidase would cause the conformational change of the enzyme.

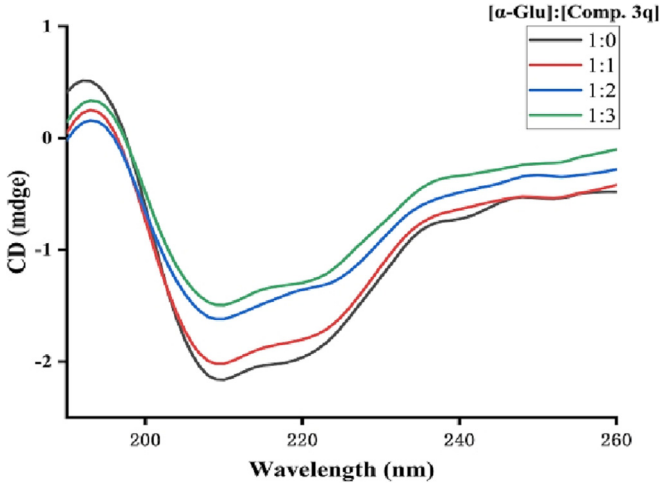

Fig. 5 CD spectra of α-glucosidase and compound **3q** system.

2.6. CD spectra assay

The CD spectra of protein could reflect its secondary structure content. The CD spectra of α-glucosidase appeared two negative bands at 210 and 222 nm, that were the typical features of α-helixes (Fig. 5). Treatment with compound **3q** lead to the obviously reduction of negative bands intensity (Fig. 5). The secondary structure content change of α-glucosidase caused by compound **3q** was also obtained (Table 3). Compound **3q** (molar ratios: 3:1) caused a decrease in the content of the α-helix (from 11.00 to 9.40 %), β-turn (from 20.20 to 19.50 %), and random coil (from 33.30 to 32.50 %), while an increase in β-Sheet (from 30.20 to 34.40 %), respectively. These results suggested that the binding of compound **3q** to α-glucosidase altered the conformation followed by the active center transfer or the shutdown.

2.7. Molecular docking

Finally, the binding mode of compound **3q** with α-glucosidase was simulated using molecular docking software and the docking results was presented in Fig. 6. Compound **3q** was anchored into the middle side of active site of α-glucosidase with naphthalene ring part locating outside of the active site and carboxyl

Table 3 The secondary structures contents of α-glucosidase with compound **3q** system.

Molar ratio [α-Glu]:[Comp.20]	α-Helix (%)	β-Sheet (%)	β-Turn (%)	Rndm Coil (%)
1:0	11.00	30.20	20.20	33.30
1:1	10.40	30.30	20.20	33.70
1:2	9.50	33.20	19.7	32.90
1:3	9.40	34.40	19.50	32.50

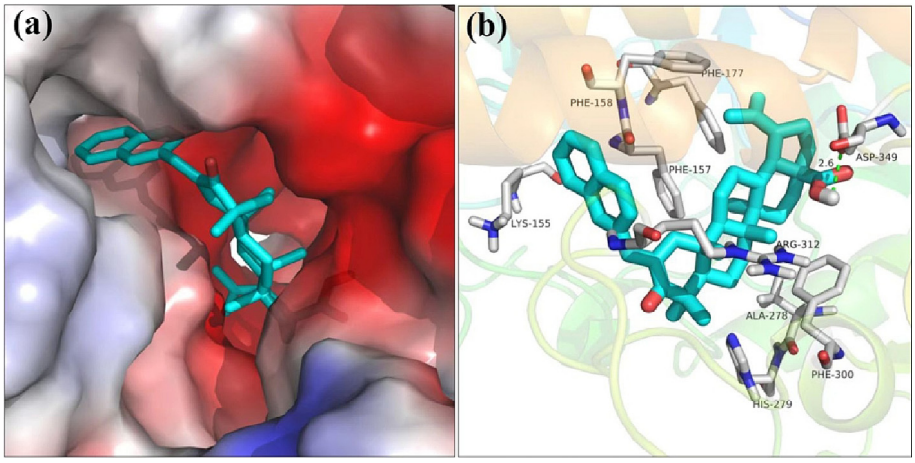

Fig. 6 The molecular docking of α-glucosidase with compound **3q**.

Table 4 The physicochemical parameters of selected betulinic acid derivatives.

Compound	MW (g/mol)	N[a]	RB	HBA	HBD	TPSA (Å^2)	Log$P_{o/w}$	WS
3a	542.79	40	3	3	1	54.37	7.63	Poorly soluble
3c	598.90	44	4	3	2	54.37	8.77	Poorly soluble
3f	577.24	41	3	3	1	54.37	8.11	Poorly soluble
3g	610.79	44	4	6	1	54.37	8.65	Poorly soluble
3i	567.80	42	3	4	1	78.16	7.40	Poorly soluble
3j	618.89	46	4	3	1	54.37	8.76	Insoluble
3p	634.89	47	5	4	1	63.60	8.78	Insoluble
3q	592.85	44	3	3	1	54.37	8.47	Insoluble
3r	548.82	39	3	3	1	82.61	7.62	Poorly soluble
3u	548.84	40	3	3	1	54.37	7.98	Poorly soluble

MW (Molecular Weight), N[a] (Num. heavy atoms), RB (Rotatable bonds), HBA (H-Bond acceptor atoms), HBD (H-Bond donor atoms), TPSA (Topology polar surface area), WS (Water solubility).

moiety of betulinic acid nesting inside (Fig. 6a). The detailed interaction was investigated and found that the carboxyl moiety formed hydrogen bonds with Asp349 (bond length: 2.6 Å), which was reported as the key interaction between compound and protein. At the same time, compound **3q** made hydrophobic interactions with Phe157, Phe158, Phe177, Als278, and Phe300. Mentioned above interactions helped compound **3q** to bind into the active site of the α-glucosidase.

2.8. Physicochemical parameters assay

The physicochemical parameters of betulinic acid derivatives **3a**, **3c**, **3f**, **3g**, **3i**, **3j**, **3p**, **3q**, **3r**, and **3u** were further assessed using SwissADME software (https://www.swissadme.ch/index.php) to assess the drug-like profile and the results were listed in Table 4. Overall, the studied betulinic acid derivatives presented favourable drug-likeness profile, in spite of the molecular weight of each derivative was higher than 500, due to the high molecular weight of betulinic acid (456.7). In particular, RB, HBA, and HBD values (RB < 10, HBA < 5, HBD < 10) were compatible with good TPSA permeability (TPSA < 90 $Å^2$). The p*hysicochemical parameters assay* results would contribute to the further structural modification of betulinic acid and in-depth pharmacology research.

3. Conclusion

In conclusion, a series of betulinic acid derivatives (**3a** ∼ **3u**, **4a** ∼ **4e**) were synthesized and assayed their α-glucosidase inhibitory activity. All synthesized derivatives exhibited stronger anti-α-glucosidase activities than betulinic acid and acarbose. Compound **3q** presented the outstanding inhibitory activity (IC_{50}: 0.56 ± 0.05 μM). Compound **3q** was revealed as a reversible and noncompetitive α-glucosidase inhibitor. 3D fluorescence and CD spectra were used to assay the effect of compound **3q** on the conformational and secondary structure content change of α-glucosidase. Molecular docking was also used to simulate the interaction between compound **3q** and α-glucosidase. Overall, betulinic acid derivatives could be used as the leading compound in the management of Type 2 diabetes.

4. Experimental

4.1. General procedure for preparation of BA derivatives

*4.1.1. **General procedure for preparation of BA derivatives 3a ∼ 3u***

2-Iodoxybenzoic acid (2.46 g 4.4 mol) was added slowly to a solution of BA (2 g, 2.2 mmol) in dry DMSO (25 mL) at 0 °C. The mixture was stirred until TLC indicated completed consumption of BA. The reaction was quenched with water and extracted with ethyl acetate, followed by evaporation under reduced pressure to give betulonic acid **2**. To a solution of betulonic acid **2** (1 mmol) and NaOH (6 mmol) in ethanol (10 mL) at 0 °C was added substituted aldehydes (3 mmol). After reaction completed, the mixture was quenched by addition of dilute hydrochloric acid (pH = 4 ∼ 5), the resulting solution was extracted with ethyl acetate. The combined organic extract was washed with saturated NaCl, dried Na_2SO_4, and concentrated in vacuo. Final purification of the residue by column chromatography afforded BA derivatives **3a** ∼ **3u**.

(3a, $C_{37}H_{50}O_3$). White sold; Yield 66 %; m. p. 182 – 185 °C; ^{1}H NMR (500 MHz, Chloroform - *d*) δ 7.51–7.46 (m, 1H), 7.41 (d, *J* = 5.8 Hz, 4H), 7.33 (tt, *J* = 5.5, 2.6 Hz, 1H), 4.76 (d, *J* = 2.2 Hz, 1H), 4.65 (t, *J* = 1.9 Hz, 1H), 3.03 (ddd, *J* = 22.3, 13.6, 3.2 Hz, 2H), 2.34–2.18 (m, 3H), 1.99 (q, *J* = 8.3, 7.9 Hz, 2H), 1.73 (s, 3H), 1.67 (t, *J* = 11.4 Hz, 1H), 1.55–1.38 (m, 12H), 1.33–1.22 (m, 2H), 1.13 (d, *J* = 10.8 Hz, 7H), 1.03 (s, 6H), 0.97 (s, 3H), 0.79 (s, 3H); ^{13}C NMR (126 MHz, $CDCl_3$) δ 207.45, 181.41, 149.70, 136.54, 135.09, 133.31, 129.48, 127.61, 127.58, 108.80, 55.58, 51.91, 48.28, 47.55, 45.96, 44.31, 43.58, 41.63, 39.64, 37.58, 36.16, 35.61, 32.18, 31.18, 29.74, 28.80, 28.61, 24.73, 21.47, 20.77, 19.48, 18.64, 14.95, 14.60, 13.75.

(3b, $C_{38}H_{52}O_3$). White sold; Yield 70 %; m. p. 289.7–290.5 °C; ^{1}H NMR (500 MHz, Chloroform-*d*) δ 7.47 (d, *J* = 2.6 Hz, 1H), 7.33 (d, *J* = 8.0 Hz, 2H), 7.22 (d, *J* = 7.9 Hz, 2H), 4.76 (d, *J* = 2.2 Hz, 1H), 4.65 (t, *J* = 1.9 Hz, 1H), 3.09–2.98 (m, 2H), 2.38 (s, 3H), 2.33–2.17 (m, 3H), 2.06–1.94 (m, 2H), 1.73 (s, 3H), 1.67 (t, *J* = 11.4 Hz, 1H), 1.57–1.38 (m, 11*H*), 1.33–1.20 (m, 4H), 1.14 (s, 3H), 1.11 (s, 3H), 1.03 (s, 3H), 0.97 (s, 3H), 0.90–0.81 (m, 1H), 0.78 (s, 3H); ^{13}C NMR (126 MHz, $CDCl_3$) δ 208.38, 182.45, 150.69, 138.79, 137.66, 133.39, 133.26, 130.57, 129.35, 109.78, 56.59, 52.86, 49.28, 48.58, 46.97, 45.23, 44.66, 42.62, 40.63, 38.58, 37.16, 36.57, 33.18, 32.19, 30.74, 29.81, 29.65, 25.74, 22.46, 21.77, 21.53, 20.48, 19.64, 15.95, 15.60, 14.75.

(3c, $C_{41}H_{58}O_3$). White sold; Yield 84 %; m. p. 261 – 263 °C; ^{1}H NMR (500 MHz, Chloroform-*d*) δ 7.48–7.43 (m, 3H), 7.40 (d, *J* = 8.5 Hz, 2H), 4.78 (d, *J* = 2.2 Hz, 1H), 4.67 (dd, *J* = 3.3, 1.7 Hz, 1H), 3.11–3.00 (m, 2H), 2.33–2.21 (m, 3H), 2.06–1.94 (m, 2H), 1.74 (s, 3H), 1.68 (t, *J* = 11.4 Hz, 1H), 1.59–1.49 (m, 3H), 1.49–1.40 (m, 7H), 1.35 (s, 9H), 1.33 (s, 1H), 1.30–1.25 (m, 3H), 1.14 (s, 3H), 1.11 (s, 3H), 1.04 (s, 3H), 0.98 (s, 3H), 0.88 (t, *J* = 6.9 Hz, 2H), 0.79 (s, 3H); ^{13}C NMR (126 MHz, $CDCl_3$) δ 208.46, 182.40, 151.94, 150.85, 137.47, 133.40, 133.24, 130.54, 125.66, 109.69, 56.62, 52.79, 49.28, 48.59, 46.96, 45.17, 44.82, 42.63, 40.64, 38.59, 37.16, 36.54, 34.93, 33.17, 32.19, 31.73, 31.48, 31.35, 30.79, 29.82, 29.73, 25.79, 22.80, 22.42, 21.81, 20.51, 19.70, 16.02, 15.60, 14.75, 14.27.

(3d, $C_{38}H_{52}O_4$). White sold; Yield 73 %; m. p. 271.9–274.2 °C; ^{1}H NMR (500 MHz, Chloroform-*d*) δ 7.47 (t, *J* = 2.0 Hz, 1H), 7.41 (d, *J* = 2.1 Hz, 1H), 7.40 (d, *J* = 2.3 Hz, 1H), 6.95 (d, *J* = 2.0 Hz, 1H), 6.94 (d, *J* = 2.1 Hz, 1H), 4.77 (d, *J* = 2.3 Hz, 1H), 4.69–4.64 (m, 1H), 3.85 (s, 3H), 3.03 (ddd, *J* = 15.5, 6.3, 4.4 Hz, 2H), 2.35–2.16 (m, 3H), 2.06–1.96 (m, 2H), 1.74 (s, 4H), 1.68 (t, *J* = 11.4 Hz, 1H), 1.58–1.48 (m, 4H), 1.48–1.40 (m, 6H), 1.34–1.22 (m, 2H), 1.14 (s, 4H), 1.11 (s, 3H), 1.03 (s, 3H), 0.97 (s, 3H), 0.79 (s, 3H); ^{13}C NMR (126 MHz, $CDCl_3$) δ 208.30, 182.19, 159.94, 150.78, 137.45, 132.37, 132.07, 128.79, 114.13, 109.75, 56.59, 55.45, 52.76, 49.30, 48.63, 46.97, 45.13, 44.80, 42.63, 40.64, 38.59, 37.16, 36.52, 33.18, 32.19, 30.76, 29.81, 29.75, 25.78, 22.45, 21.81, 20.51, 19.67, 15.99, 15.60, 14.76.

(3e, $C_{37}H_{49}FO_3$). White sold; Yield 72 %; m. p. 297.3–300.7 °C; ^{1}H NMR (500 MHz, Chloroform-*d*) δ 7.44 (t, *J* = 2.0 Hz, 1H), 7.42–7.37 (m, 2H), 7.13–7.07 (m, 2H), 4.76 (d, *J* = 2.2 Hz, 1H), 4.66 (dd, *J* = 2.3, 1.4 Hz, 1H), 3.05–

2.96 (m, 2H), 2.33–2.21 (m, 2H), 2.18 (dd, J = 16.7, 2.9 Hz, 1H), 2.04–1.94 (m, 2H), 1.73 (s, 4H), 1.67 (t, J = 11.4 Hz, 1H), 1.56–1.40 (m, 12H), 1.34–1.22 (m, 2H), 1.13 (d, J = 12.2 Hz, 7H), 1.03 (s, 3H), 0.97 (s, 3H), 0.78 (s, 3H); ^{13}C NMR (126 MHz, $CDCl_3$) δ 208.25, 182.41, 163.64, 161.65, 150.66, 136.36, 133.93, 132.36, 132.29, 132.22, 132.20, 115.80, 115.63, 109.82, 56.58, 52.86, 49.27, 48.55, 46.96, 45.27, 44.52, 42.62, 40.63, 38.57, 37.15, 36.59, 33.15, 32.17, 30.72, 29.80, 29.61, 25.72, 22.45, 21.78, 20.46, 19.63, 15.94, 15.60, 14.74.

(3f, $C_{37}H_{49}ClO_3$). White sold; Yield 59 %; m. p. 306.5–308.9 °C; ^{1}H NMR (500 MHz, Chloroform-*d*) δ 7.43 (dd, J = 3.0, 1.5 Hz, 1H), 7.39 (d, J = 2.1 Hz, 1H), 7.38 (d, J = 2.3 Hz, 1H), 7.34 (d, J = 8.7 Hz, 2H), 4.76 (d, J = 2.2 Hz, 1H), 4.67–4.64 (m, 1H), 3.06–2.95 (m, 2H), 2.34–2.21 (m, 2H), 2.20–2.15 (m, 1H), 2.02–1.96 (m, 2H), 1.73 (s, 4H), 1.67 (t, J = 11.4 Hz, 1H), 1.54–1.43 (m, 12H), 1.27 (dq, J = 16.5, 4.7 Hz, 4H), 1.14 (s, 3H), 1.12 (s, 3H), 1.03 (s, 3H), 0.97 (s, 3H), 0.78 (s, 3H); ^{13}C NMR (126 MHz, $CDCl_3$) δ 208.20, 150.60, 136.16, 134.83, 134.50, 134.48, 131.63, 128.86, 109.87, 77.41, 77.36, 77.16, 76.91, 56.57, 52.90, 49.27, 48.55, 46.96, 45.33, 44.52, 42.63, 40.64, 38.57, 37.16, 36.62, 33.16, 32.18, 30.72, 29.84, 29.80, 29.57, 25.70, 22.47, 21.78, 20.45, 19.62, 15.94, 15.60, 14.75.

(3 g, $C_{38}H_{49}F_3O_3$). White sold; Yield 89 %; m. p. 283.0–283.4 °C; ^{1}H NMR (500 MHz, Chloroform-*d*) δ 7.67 (s, 1H), 7.65 (s, 1H), 7.50 (s, 1H), 7.49 (s, 1H), 7.48–7.45 (m, 1H), 4.76 (d, J = 2.3 Hz, 1H), 4.65 (t, J = 1.8 Hz, 1H), 3.01 (ddd, J = 16.3, 6.6, 3.1 Hz, 2H), 2.33–2.17 (m, 3H), 2.06–1.94 (m, 2H), 1.72 (s, 4H), 1.66 (t, J = 11.4 Hz, 1H), 1.52–1.41 (m, 11*H*), 1.30–1.24 (m, 2H), 1.14 (s, 3H), 1.13 (s, 3H), 1.02 (s, 3H), 0.97 (s, 3H), 0.88 (t, J = 6.9 Hz, 1H), 0.79 (s, 3H); ^{13}C NMR (126 MHz, $CDCl_3$) δ 208.14, 182.33, 150.58, 139.57, 136.41, 135.66, 130.36, 125.56, 125.53, 125.50, 125.47, 109.87, 56.57, 52.98, 49.26, 48.51, 46.96, 45.44, 44.44, 42.64, 40.65, 38.57, 37.15, 36.69, 33.15, 32.17, 31.73, 30.72, 29.79, 29.50, 25.68, 22.80, 22.49, 21.78, 20.44, 19.62, 15.95, 15.61, 14.74, 14.27.

(3 h, $C_{37}H_{49}NO_5$). White sold; Yield 53 %; m. p. 214.5–216.7 °C; ^{1}H NMR (500 MHz, Chloroform-*d*) δ 8.26 (d, J = 8.8 Hz, 2H), 7.53 (d, J = 8.8 Hz, 2H), 7.47 (q, J = 1.5 Hz, 1H), 4.75 (d, J = 2.2 Hz, 1H), 4.65 (t, J = 1.8 Hz, 1H), 3.05–2.95 (m, 2H), 2.33–2.18 (m, 3H), 1.98 (q, J = 7.7, 6.9 Hz, 2H), 1.71 (s, 3H), 1.78–1.61 (m, 2H), 1.54–1.38 (m, 8H), 1.34–1.21 (m, 4H), 1.14 (d, J = 7.0 Hz, 7H), 1.02 (s, 3H), 0.97 (s, 3H), 0.78 (s, 3H); ^{13}C NMR (126 MHz, $CDCl_3$) δ 207.91, 182.41, 150.47, 147.20, 142.60, 137.88, 134.62, 130.77, 123.82, 109.94, 56.54, 52.97, 49.23, 48.48, 46.95, 45.51, 44.52, 42.64, 40.64, 38.54, 37.14, 36.73, 33.12, 32.14, 30.67, 29.77, 29.46, 25.63, 22.49, 21.79, 20.41, 19.59, 15.98, 15.59, 14.72.

(3i, $C_{38}H_{49}NO_3$). White sold; Yield 58 %; m. p. 292.2–295.5 °C; ^{1}H NMR (500 MHz, Chloroform-*d*) δ 7.72–7.66 (m, 2H), 7.48 (d, J = 8.3 Hz, 2H), 7.45–7.37 (m, 1H), 4.76 (d, J = 2.3 Hz, 1H), 4.65 (t, J = 1.8 Hz, 1H), 3.05–2.93 (m, 2H), 2.33–2.16 (m, 3H), 2.06–1.94 (m, 2H), 1.72 (s, 3H), 1.79–1.62 (m, 2H), 1.55–1.40 (m, 10*H*), 1.35–1.19 (m, 4H), 1.14 (s, 6H), 1.12 (s, 3H), 1.02 (s, 4H), 0.97 (s, 3H), 0.78 (s, 3H); ^{13}C NMR (126 MHz, $CDCl_3$) δ 207.98, 182.29, 150.57, 140.61, 137.34, 135.06, 132.32, 130.61, 118.78, 111.73, 109.87, 56.54, 52.95, 49.24, 48.49, 46.94, 45.46, 44.51, 42.64, 40.64, 38.53, 37.14, 36.70, 33.12, 32.14, 30.69, 29.77, 29.48, 25.66, 22.47, 21.79, 20.41, 19.61, 15.96, 15.58, 14.72.

(3j, $C_{43}H_{54}O_3$). White sold; Yield 66 %; m. p. 283.9–285.6 °C; ^{1}H NMR (500 MHz, Chloroform-*d*) δ 7.67–7.63 (m, 4H), 7.52 (t, J = 6.1 Hz, 3H), 7.46 (dd, J = 8.4, 6.9 Hz, 2H), 7.39–7.34 (m, 1H), 4.76 (d, J = 2.2 Hz, 1H), 4.67–4.64 (m, 1H), 3.11 (dd, J = 16.5, 1.6 Hz, 1H), 3.02 (td, J = 10.8, 4.8 Hz, 1H), 2.27 (dtd, J = 15.8, 9.0, 7.7, 3.4 Hz, 3H), 2.01 (dq, J = 15.7, 7.4 Hz, 2H), 1.73 (s, 4H), 1.67 (t, J = 11.4 Hz, 1H), 1.56–1.43 (m, 12H), 1.29–1.24 (m, 2H), 1.16 (s, 3H), 1.13 (s, 3H), 1.04 (s, 3H), 0.98 (s, 3H), 0.81 (s, 3H); ^{13}C NMR (126 MHz, $CDCl_3$) δ 208.37, 150.70, 141.23, 140.43, 137.14, 135.06, 134.30, 131.07, 129.01, 127.80, 127.23, 127.17, 109.80, 56.59, 56.56, 52.88, 49.29, 48.60, 46.96, 45.29, 44.80, 42.64, 40.65, 38.59, 37.16, 36.62, 33.19, 32.19, 30.74, 29.81, 29.68, 25.75, 22.48, 21.82, 20.50, 19.65, 16.01, 15.61, 14.77.

(3 k, $C_{39}H_{55}NO_3$). White sold; Yield 54 %; m. p. 292.2–294.8 °C; ^{1}H NMR (500 MHz, Chloroform-*d*) δ 10.62 (s, 1H), 7.48 (s, 1H), 7.41 (d, J = 8.4 Hz, 2H), 6.79 (s, 2H), 4.78 (d, J = 2.3 Hz, 1H), 4.66 (t, J = 1.9 Hz, 1H), 3.03 (s, 8H), 2.33–2.18 (m, 3H), 1.99 (q, J = 8.4 Hz, 2H), 1.77 (q, J = 7.9, 5.7 Hz, 1H), 1.74 (s, 3H), 1.68 (t, J = 11.4 Hz, 1H), 1.61–1.38 (m, 9H), 1.35–1.22 (m, 2H), 1.12 (d, J = 18.1 Hz, 7H), 1.03 (s, 3H), 0.97 (s, 3H), 0.79 (s, 3H); ^{13}C NMR (126 MHz, $CDCl_3$) δ 208.03, 182.22, 171.37, 150.91, 150.49, 138.62, 132.66, 129.41, 124.09, 111.91, 109.64, 60.56, 56.60, 52.62, 49.30, 48.71, 46.95, 45.08, 44.92, 42.61, 40.63, 40.27, 38.59, 37.16, 36.40, 33.20, 32.21, 30.79, 29.90, 29.82, 25.83, 22.44, 21.80, 21.19, 20.53, 19.70, 16.04, 15.59, 14.75, 14.32.

(3 L, $C_{38}H_{52}O_5S$). Yellow sold; Yield 71 %; m. p. 287.7–289.3 °C; ^{1}H NMR (500 MHz, Chloroform-*d*) δ 7.98–7.94 (m, 2H), 7.57–7.53 (m, 2H), 7.48–7.46 (m, 1H), 4.75 (d, J = 2.3 Hz, 1H), 4.65 (t, J = 1.8 Hz, 1H), 3.09 (s, 3H), 3.05–2.93 (m, 2H), 2.32–2.16 (m, 3H), 1.98 (q, J = 7.8, 7.1 Hz, 2H), 1.71 (s, 4H), 1.66 (t, J = 11.4 Hz, 1H), 1.55–1.38 (m, 11*H*), 1.25 (ddt, J = 12.9, 9.6, 3.4 Hz, 3H), 1.14 (d, J = 5.0 Hz, 6H), 1.02 (s, 3H), 0.96 (s, 3H), 0.78 (s, 3H); ^{13}C NMR (126 MHz, $CDCl_3$) δ 207.97, 182.32, 150.48, 141.62, 139.75, 137.48, 134.95, 130.75, 127.60, 109.96, 56.52, 53.00, 49.23, 48.47, 46.95, 45.50, 44.58, 44.38, 42.63, 40.64, 38.54, 37.14, 36.73, 33.14, 32.15, 30.67, 29.76, 29.45, 25.64, 22.50, 21.78, 20.40, 19.59, 15.95, 15.60, 14.73.

(3 m, $C_{39}H_{51}N_3O_3$). White sold; Yield 75 %; m. p. 213.1–215.6 °C;^{1}H NMR (500 MHz, Chloroform-*d*) δ 8.66 (s, 1H), 8.14 (s, 1H), 7.75 (d, J = 8.1 Hz, 2H), 7.55 (d, J = 8.2 Hz, 2H), 7.49 (s, 1H), 4.76 (d, J = 2.3 Hz, 1H), 4.64 (t, J = 1.8 Hz, 1H), 3.07–2.97 (m, 2H), 2.34–2.20 (m, 3H), 2.05–1.95 (m, 2H), 1.72 (s, 4H), 1.66 (t, J = 11.4 Hz, 1H), 1.58–1.39 (m, 12H), 1.35–1.22 (m, 3H), 1.15 (s, 3H), 1.13 (s, 3H), 1.03 (s, 3H), 0.97 (s, 3H), 0.79 (s, 3H); ^{13}C NMR (126 MHz, $CDCl_3$) δ 208.09, 181.79, 152.53, 150.64, 136.41, 136.19, 135.70, 135.54, 131.74, 119.97, 109.84, 77.37, 56.51, 52.93, 49.25, 48.57, 46.97, 45.39, 44.57, 42.64, 40.64, 38.55, 37.16, 36.66, 33.17, 32.20, 30.70, 29.79, 29.55, 25.71, 22.50, 21.80, 20.44, 19.61, 15.96, 15.61, 14.74.

(3n, $C_{39}H_{54}O_5$). White sold; Yield 61 %; m. p. 200.7–202.2 °C; ^{1}H NMR (500 MHz, Chloroform-*d*) δ 7.44 (t, J = 2.0 Hz, 1H), 7.07 (dd, J = 8.4, 1.8 Hz, 1H), 6.98–6.90 (m, 2H), 4.64 (q, J = 1.8 Hz, 1H), 3.92 (d, J = 2.5 Hz, 3H), 3.88 (d, J = 1.7 Hz, 3H), 3.11–2.96 (m, 2H), 2.33–2.16 (m,

3H), 2.05–1.94 (m, 2H), 1.58–1.37 (m, 12H), 1.34–1.21 (m, 12H), 1.12 (dd, J = 12.5, 1.9 Hz, 7H), 1.03 (d, J = 1.6 Hz, 3H), 0.97 (d, J = 3.3 Hz, 3H), 0.91–0.84 (m, 5H), 0.79 (d, J = 2.1 Hz, 3H); ^{13}C NMR (126 MHz, $CDCl_3$) δ 208.23, 150.67, 149.54, 148.72, 137.56, 132.60, 129.03, 123.12, 114.50, 111.07, 109.76, 76.91, 76.91, 56.60, 56.58, 56.03, 56.00, 52.79, 49.27, 48.70, 46.95, 45.19, 44.83, 42.62, 40.63, 38.61, 37.15, 36.51, 33.19, 32.17, 30.73, 29.82, 29.69, 25.73, 22.45, 21.85, 20.47, 19.64, 16.02, 15.61, 14.77.

(3o, $C_{40}H_{56}O_6$). White sold; Yield 72 %; m. p. 233.6–235.9 °C; ^{1}H NMR (500 MHz, Chloroform-*d*) δ 7.48–7.35 (m, 1H), 6.64 (s, 2H), 4.73 (d, J = 2.2 Hz, 1H), 4.62 (t, J = 1.7 Hz, 1H), 3.88 (d, J = 14.7 Hz, 9H), 3.09 (dd, J = 16.3, 1.6 Hz, 1H), 3.00 (td, J = 10.7, 5.0 Hz, 1H), 2.33–2.22 (m, 2H), 2.17 (dt, J = 16.1, 2.2 Hz, 1H), 2.03–1.95 (m, 2H), 1.75 (d, J = 13.4 Hz, 1H), 1.70 (s, 3H), 1.64 (t, J = 11.4 Hz, 1H), 1.55–1.38 (m, 12H), 1.38–1.20 (m, 2H), 1.13 (d, J = 4.1 Hz, 6H), 1.01 (s, 3H), 0.97 (s, 3H), 0.82 (s, 3H); ^{13}C NMR (126 MHz, $CDCl_3$) δ 208.26, 182.24, 153.03, 150.29, 138.58, 137.50, 133.91, 131.61, 109.92, 107.78, 61.09, 56.54, 56.31, 52.96, 49.20, 48.76, 46.93, 45.41, 44.54, 42.60, 40.64, 38.58, 37.11, 36.62, 33.20, 32.14, 30.65, 29.82, 29.48, 25.58, 22.48, 21.88, 20.40, 19.55, 16.04, 15.63, 14.78.

(3p, $C_{43}H_{54}O_4$). White sold; Yield 68 %; m. p. 269.2–269.9 °C; ^{1}H NMR (500 MHz, Chloroform-*d*) δ 7.49–7.45 (m, 1H), 7.44–7.35 (m, 4H), 7.19–7.14 (m, 1H), 7.09–7.05 (m, 2H), 7.04–6.99 (m, 2H), 4.77 (d, J = 2.3 Hz, 1H), 4.65 (t, J = 1.8 Hz, 1H), 3.03 (ddd, J = 15.4, 6.6, 3.1 Hz, 2H), 2.34–2.17 (m, 3H), 2.07–1.95 (m, 2H), 1.72 (s, 4H), 1.67 (t, J = 11.4 Hz, 1H), 1.58–1.38 (m, 11*H*), 1.37–1.22 (m, 2H), 1.15 (s, 3H), 1.11 (s, 3H), 1.03 (s, 3H), 0.98 (s, 3H), 0.90–0.83 (m, 1H), 0.80 (s, 3H); ^{13}C NMR (126 MHz, $CDCl_3$) δ 208.28, 182.46, 158.08, 156.35, 150.65, 136.95, 132.99, 132.34, 130.80, 130.05, 124.15, 119.89, 118.16, 109.82, 56.58, 52.78, 49.27, 48.59, 46.97, 45.18, 44.77, 42.62, 40.63, 38.58, 37.16, 36.53, 33.16, 32.18, 30.74, 29.80, 29.72, 25.75, 22.44, 21.80, 20.50, 19.64, 15.99, 15.60, 14.74.

(3q, $C_{41}H_{52}O_3$). White sold; Yield 86 %; m. p. 265.8–266.9 °C; ^{1}H NMR (500 MHz, Chloroform-*d*) δ 7.93–7.84 (m, 4H), 7.69 (d, J = 2.7 Hz, 1H), 7.59–7.51 (m, 3H), 4.78 (d, J = 2.2 Hz, 1H), 4.67 (t, J = 1.9 Hz, 1H), 3.18 (dd, J = 16.2, 1.6 Hz, 1H), 3.04 (td, J = 10.7, 4.7 Hz, 1H), 2.36–2.22 (m, 3H), 2.09–1.97 (m, 2H), 1.75 (s, 4H), 1.69 (t, J = 11.4 Hz, 1H), 1.62–1.40 (m, 11*H*), 1.29 (ddd, J = 13.2, 9.2, 3.4 Hz, 2H), 1.19 (d, J = 3.5 Hz, 6H), 1.06 (s, 3H), 0.99 (s, 3H), 0.83 (s, 3H); ^{13}C NMR (126 MHz, $CDCl_3$) δ 208.44, 182.46, 150.53, 137.74, 134.57, 133.70, 133.25, 133.07, 130.51, 128.60, 128.10, 127.76, 127.37, 126.90, 126.49, 109.85, 56.57, 52.99, 49.28, 48.53, 46.95, 45.38, 44.48, 42.62, 40.64, 38.54, 37.14, 36.74, 33.17, 32.18, 30.73, 29.80, 29.58, 25.66, 22.53, 21.74, 20.47, 19.62, 15.95, 15.61, 14.76.

(3r, $C_{35}H_{48}O_3S$). White sold; Yield 56 %; m. p. 243.5–246.2 °C; ^{1}H NMR (500 MHz, Chloroform-*d*) δ 7.71 (t, J = 2.2 Hz, 1H), 7.52 (d, J = 5.0 Hz, 1H), 7.31 (d, J = 3.6 Hz, 1H), 7.13 (dd, J = 5.1, 3.7 Hz, 1H), 4.79 (d, J = 2.2 Hz, 1H), 4.67 (d, J = 2.0 Hz, 1H), 3.04 (ddd, J = 16.9, 9.5, 3.3 Hz, 2H), 2.34–2.25 (m, 2H), 2.18–2.11 (m, 1H), 2.07–1.95 (m, 2H), 1.81 (dq, J = 12.9, 3.5 Hz, 1H), 1.74 (s, 3H), 1.71–1.63 (m, 2H), 1.60–1.33 (m, 11*H*), 1.27 (dt, J = 12.2, 2.7 Hz, 2H), 1.15 (s, 3H), 1.08 (s, 3H), 1.04 (s, 3H), 0.99 (s, 3H), 0.83 (s, 3H); ^{13}C NMR (126 MHz, $CDCl_3$) δ 207.77, 182.52, 150.64, 139.58, 132.75, 131.18, 130.43, 129.83, 127.70, 109.84, 56.61, 52.54, 49.28, 48.75, 47.00, 45.20, 44.99, 42.61, 40.59, 38.61, 37.15, 36.49, 33.09, 32.18, 30.76, 29.84, 25.77, 22.32, 21.90, 20.54, 19.64, 16.46, 15.54, 14.79.

(3 s, $C_{35}H_{48}O_4$). White sold; Yield 73 %; m. p. 280.7–283.2 °C; ^{1}H NMR (500 MHz, Chloroform-*d*) δ 7.57 (d, J = 1.7 Hz, 1H), 7.30 (d, J = 1.2 Hz, 1H), 6.59 (d, J = 3.5 Hz, 1H), 6.50 (dd, J = 3.5, 1.8 Hz, 1H), 4.79 (d, J = 2.3 Hz, 1H), 4.67 (t, J = 1.9 Hz, 1H), 3.13 (dd, J = 17.5, 1.8 Hz, 1H), 3.05 (td, J = 10.7, 4.7 Hz, 1H), 2.34–2.23 (m, 2H), 2.22–2.14 (m, 1H), 2.08–1.95 (m, 2H), 1.74 (s, 4H), 1.69 (t, J = 11.4 Hz, 1H), 1.58–1.32 (m, 9H), 1.27 (dt, J = 11.8, 2.5 Hz, 3H), 1.14 (s, 4H), 1.08 (s, 3H), 1.03 (s, 3H), 0.99 (s, 3H), 0.82 (s, 3H); ^{13}C NMR (126 MHz, $CDCl_3$) δ 207.68, 182.32, 152.74, 150.77, 144.55, 131.34, 124.34, 115.57, 112.34, 109.78, 56.61, 52.65, 49.29, 48.58, 46.99, 44.98, 44.87, 42.63, 40.60, 38.64, 37.17, 36.07, 33.16, 32.19, 30.76, 29.83, 29.80, 25.81, 22.35, 21.85, 20.52, 19.65, 16.36, 15.58, 14.76.

(3 t, $C_{36}H_{49}NO_3$). White sold; Yield 87 %; m. p. 239.9–242.6 °C; ^{1}H NMR (500 MHz, Chloroform-*d*) δ 8.73 (dd, J = 4.9, 1.8 Hz, 1H), 7.72 (td, J = 7.7, 1.9 Hz, 1H), 7.43–7.35 (m, 2H), 7.23–7.17 (m, 1H), 4.76 (d, J = 2.6 Hz, 1H), 4.64 (t, J = 1.9 Hz, 1H), 3.46 (dd, J = 17.8, 1.9 Hz, 1H), 3.03 (td, J = 10.7, 4.7 Hz, 1H), 2.43–2.35 (m, 1H), 2.32–2.22 (m, 2H), 1.99 (q, J = 8.4, 8.0 Hz, 2H), 1.72 (s, 4H), 1.66 (t, J = 11.3 Hz, 1H), 1.61–1.36 (m, 11*H*), 1.34–1.21 (m, 3H), 1.15 (s, 3H), 1.11 (s, 3H), 1.02 (s, 3H), 0.97 (s, 3H), 0.79 (s, 3H); ^{13}C NMR (126 MHz, $CDCl_3$) δ 209.01, 182.18, 155.42, 150.76, 149.46, 138.96, 136.56, 134.23, 126.72, 122.47, 109.73, 56.57, 52.94, 49.29, 48.31, 46.98, 45.44, 44.90, 42.64, 40.59, 38.59, 37.16, 36.42, 33.16, 32.21, 30.76, 29.82, 29.50, 25.72, 22.38, 21.79, 20.49, 19.62, 16.08, 15.59, 14.75.

(3u, $C_{37}H_{56}O_3$). White sold; Yield 95 %; m. p. 284.7–285.8 °C; ^{1}H NMR (500 MHz, Chloroform-*d*) δ 6.43 (dq, J = 9.8, 1.4 Hz, 1H), 4.76 (d, J = 2.2 Hz, 1H), 4.64–4.62 (m, 1H), 3.03 (td, J = 10.8, 4.9 Hz, 1H), 2.70 (dd, J = 15.9, 1.5 Hz, 1H), 2.35–2.23 (m, 3H), 2.14 (dt, J = 10.3, 3.7 Hz, 1H), 2.07–1.94 (m, 2H), 1.85 (dd, J = 15.8, 2.6 Hz, 1H), 1.81–1.73 (m, 1H), 1.71 (s, 4H), 1.67 (s, 1H), 1.54 (dt, J = 23.7, 9.8 Hz, 4H), 1.43 (d, J = 4.0 Hz, 8H), 1.34 (dd, J = 11.9, 3.9 Hz, 1H), 1.32–1.08 (m, 5H), 1.05 (d, J = 2.6 Hz, 7H), 1.01 (s, 3H), 0.98 (s, 4H), 0.77 (s, 3H); ^{13}C NMR (126 MHz, $CDCl_3$) δ 208.28, 182.42, 150.61, 146.67, 131.86, 109.89, 77.37, 56.56, 53.19, 49.28, 48.51, 47.01, 45.26, 42.63, 42.24, 40.62, 38.65, 37.19, 37.03, 36.27, 33.32, 32.20, 31.82, 31.73, 30.66, 29.80, 29.31, 26.02, 25.76, 25.70, 22.41, 21.73, 20.42, 19.53, 15.75, 15.67, 14.74.

4.1.2. General procedure for preparation of BA derivatives ***4a*** $\sim$ ***4b***

To a solution of dry DMF (15 mL) containing derivative **3q** (0.4 mmol) and K_2CO_3 (0.8 mmol), CH_3I or benzyl bromide (1.2 mmol) was added. The mixture was stirred at room temperature until the reaction completed. After quenched by water, the solution was extracted with ethyl acetate, followed by the wash with saturated NaCl, dry with Na_2SO_4, concentration in vacuo, and subsequently purification with column chromatography to yield BA derivatives **4a** $\sim$ **4b**.

(4a, $C_{42}H_{54}O_3$). White sold; Yield 75 %; m. p. 147.9–149.6 °C; ^{1}H NMR (500 MHz, Chloroform-*d*) δ 7.91–7.82 (m, 4H), 7.67–7.64 (m, 1H), 7.53 (ddd, J = 12.4, 7.4, 2.5 Hz,

3H), 4.75 (d, J = 2.2 Hz, 1H), 4.64 (t, J = 1.9 Hz, 1H), 3.67 (s, 3H), 3.15 (dd, J = 16.2, 1.6 Hz, 1H), 3.00 (td, J = 10.8, 4.4 Hz, 1H), 2.31 (d, J = 2.9 Hz, 1H), 2.29–2.22 (m, 3H), 1.95–1.85 (m, 2H), 1.72 (s, 4H), 1.63 (t, J = 11.4 Hz, 1H), 1.56–1.32 (m, 10*H*), 1.29–1.20 (m, 2H), 1.17 (s, 3H), 1.15 (s, 3H), 1.10 (dd, J = 13.1, 4.1 Hz, 1H), 1.02 (s, 3H), 0.96 (s, 3H), 0.81 (s, 3H); ^{13}C NMR (126 MHz, $CDCl_3$) δ 208.43, 176.76, 150.74, 137.66, 134.66, 133.72, 133.25, 133.07, 130.50, 128.61, 128.11, 127.77, 127.38, 126.89, 126.49, 109.74, 56.71, 53.03, 51.48, 49.49, 48.61, 47.00, 45.39, 44.49, 42.60, 40.65, 38.40, 37.06, 36.75, 33.21, 32.19, 30.78, 29.78, 29.59, 25.71, 22.59, 21.80, 20.53, 19.65, 15.97, 15.56, 14.78.

(4b, $C_{48}H_{58}O_3$). White sold; Yield 79 %; m. p. 154.6–157.5 °C; ^{1}H NMR (500 MHz, Chloroform-*d*) δ 7.91–7.82 (m, 4H), 7.65 (d, J = 2.6 Hz, 1H), 7.52 (ddd, J = 9.7, 7.2, 2.4 Hz, 3H), 7.40–7.29 (m, 5H), 5.15 (d, J = 12.3 Hz, 1H), 5.09 (d, J = 12.3 Hz, 1H), 4.74 (d, J = 2.3 Hz, 1H), 4.63 (t, J = 2.0 Hz, 1H), 3.14 (d, J = 16.1 Hz, 1H), 3.02 (td, J = 11.0, 4.7 Hz, 1H), 2.34–2.19 (m, 3H), 1.96–1.83 (m, 2H), 1.71 (s, 4H), 1.63 (t, J = 11.3 Hz, 1H), 1.53–1.34 (m, 9H), 1.27 (dtd, J = 31.6, 13.4, 3.8 Hz, 2H), 1.17 (s, 4H), 1.15 (s, 3H), 1.08 (dd, J = 13.0, 4.1 Hz, 1H), 1.00 (s, 3H), 0.88 (t, J = 6.8 Hz, 1H), 0.79 (s, 6H); ^{13}C NMR (126 MHz, $CDCl_3$) δ 208.44, 175.90, 150.74, 137.66, 136.56, 134.67, 133.72, 133.25, 133.06, 130.49, 128.63, 128.61, 128.42, 128.23, 128.11, 127.77, 127.38, 126.89, 126.49, 109.73, 65.91, 56.68, 53.03, 49.48, 48.61, 46.96, 45.39, 44.48, 42.59, 40.62, 38.34, 37.03, 36.73, 33.20, 32.13, 30.75, 29.66, 29.58, 25.74, 22.59, 21.80, 20.52, 19.65, 15.97, 15.42, 14.74.

4.1.3. General procedure for preparation of BA derivatives ***4c*** ∼ ***4e***

To a solution of dry DMF (6 mL) containing derivative **3q** (0.4 mmol), HATU (0.4 mmol), and DIPEA (0.8 mmol), piperazines or amines (0.8 mmol) are added. After the reaction was completed, the mixture was quenched by water and extracted with ethyl acetate, followed by the wash with saturated NaCl, dry with Na_2SO_4, concentration in vacuo, and subsequently purification with column chromatography to yield BA derivatives **4c** ∼ **4e**.

(4c, $C_{51}H_{64}N_2O_2$). White sold; Yield 80 %; m. p. 277.2–279.5 °C; ^{1}H NMR (500 MHz, Chloroform-*d*) δ 7.91–7.82 (m, 4H), 7.64 (s, 1H), 7.56–7.48 (m, 3H), 7.29 (t, J = 7.8 Hz, 2H), 6.93 (dd, J = 14.7, 7.6 Hz, 3H), 4.75 (d, J = 2.3 Hz, 1H), 4.62 (s, 1H), 3.77 (s, 4H), 3.51–3.42 (m, 1H), 3.15 (t, J = 11.3 Hz, 5H), 3.04–2.91 (m, 2H), 2.33–2.24 (m, 1H), 2.17 (dt, J = 13.7, 3.5 Hz, 1H), 2.03 (dd, J = 11.2, 7.1 Hz, 1H), 1.89 (dt, J = 19.1, 8.1 Hz, 1H), 1.72 (s, 4H), 1.67–1.56 (m, 2H), 1.55–1.36 (m, 9H), 1.26 (ddt, J = 28.1, 13.5, 3.8 Hz, 2H), 1.16 (d, J = 9.7 Hz, 6H), 1.03 (s, 3H), 0.98 (s, 3H), 0.82 (s, 3H); ^{13}C NMR (126 MHz, $CDCl_3$) δ 208.53, 173.62, 151.48, 151.11, 137.63, 134.78, 133.74, 133.26, 133.07, 130.50, 129.55, 129.37, 128.62, 128.11, 127.77, 127.37, 126.87, 126.47, 120.54, 117.44, 116.46, 109.33, 54.75, 53.12, 52.73, 49.73, 48.94, 45.71, 45.40, 44.56, 42.12, 40.65, 37.08, 36.80, 36.11, 33.29, 32.63, 31.52, 29.91, 29.57, 25.87, 22.56, 22.08, 20.52, 19.98, 16.04, 15.73, 14.77, 0.14.

(4d, $C_{43}H_{57}NO_2$). White sold; Yield 72 %; m. p. 161.5–165.3 °C; ^{1}H NMR (500 MHz, Chloroform-*d*) δ 7.89–7.82 (m, 4H), 7.66–7.63 (m, 1H), 7.52 (ddd, J = 13.1, 7.4, 2.5 Hz, 3H), 5.61 (t, J = 5.7 Hz, 1H), 4.75 (d, J = 2.2 Hz, 1H), 4.62 (t, J = 1.8 Hz, 1H), 3.33 (dp, J = 13.6, 6.9 Hz, 1H), 3.25–3.19 (m, 1H), 3.19–3.12 (m, 2H), 2.53 (td, J = 12.3, 3.5 Hz, 1H), 2.28 (dd, J = 16.6, 2.9 Hz, 1H), 2.04–1.90 (m, 2H), 1.76–1.73 (m, 1H), 1.71 (s, 3H), 1.61 (d, J = 11.3 Hz, 1H), 1.59–1.55 (m, 1H), 1.55–1.51 (m, 1H), 1.49 (d, J = 7.2 Hz, 5H), 1.44 (ddd, J = 11.6, 7.5, 4.1 Hz, 2H), 1.40–1.31 (m, 1H), 1.30–1.23 (m, 1H), 1.21 (d, J = 3.4 Hz, 1H), 1.17 (s, 3H), 1.15 (s, 3H), 1.12 (t, J = 7.2 Hz, 3H), 1.07 (dd, J = 13.0, 4.1 Hz, 1H), 1.02 (s, 3H), 0.98 (s, 3H), 0.81 (s, 3H). ^{13}C NMR (126 MHz, $CDCl_3$) δ 208.47, 175.98, 151.23, 137.65, 134.70, 133.69, 133.24, 133.06, 130.49, 128.60, 128.11, 127.76, 127.34, 126.87, 126.47, 109.40, 55.60, 53.04, 50.20, 48.70, 46.82, 45.38, 44.49, 42.66, 40.73, 38.50, 37.86, 36.75, 34.20, 33.86, 33.29, 31.07, 29.57, 29.49, 25.82, 22.56, 21.85, 20.51, 19.78, 15.98, 15.74, 15.20, 14.71.

(4e, $C_{44}H_{59}NO_2$). White sold; Yield 70 %; m. p. 164.6–168.9 °C; ^{1}H NMR (500 MHz, Chloroform-*d*) δ 7.90–7.81 (m, 4H), 7.66–7.62 (m, 1H), 7.52 (ddd, J = 11.8, 7.4, 2.5 Hz, 3H), 5.61 (t, J = 5.9 Hz, 1H), 4.75 (d, J = 2.3 Hz, 1H), 4.62 (t, J = 1.8 Hz, 1H), 3.26 (dq, J = 13.3, 6.6 Hz, 1H), 3.19–3.08 (m, 3H), 2.53 (td, J = 12.4, 3.5 Hz, 1H), 2.28 (dd, J = 16.1, 2.9 Hz, 1H), 2.01–1.89 (m, 2H), 1.77–1.64 (m, 8H), 1.63–1.56 (m, 2H), 1.48 (tdd, J = 23.6, 7.7, 3.6 Hz, 10*H*), 1.30–1.18 (m, 2H), 1.16 (s, 3H), 1.15 (s, 3H), 1.02 (s, 3H), 0.98 (s, 3H), 0.92 (t, J = 7.4 Hz, 3H), 0.81 (s, 3H).^{13}C NMR (126 MHz, $CDCl_3$) δ 208.27, 175.84, 150.99, 137.42, 134.47, 133.46, 133.00, 132.82, 130.26, 128.36, 127.87, 127.52, 127.10, 126.63, 126.23, 109.16, 55.49, 52.81, 49.97, 48.48, 46.55, 45.14, 44.26, 42.43, 40.83, 40.49, 38.35, 37.62, 36.53, 33.69, 33.07, 30.84, 29.33, 29.28, 25.59, 22.98, 22.31, 21.63, 20.28, 19.55, 15.75, 15.53, 14.47, 11.37.

4.2. a-Glucosidase inhibition and kinetics assay

The α-glucosidase (from Saccharomyces cerevisiae, Sigma-Aldrich) inhibitory activity of BA derivatives was determined with acarbose and BA as control (Yang et al., 2021; Yang et al., 2021). After α-glucosidase incubated with BA derivatives for 10 min in phosphate buffered saline (0.1 M, pH 6.8), pNPG solution was added into the mixture, and the absorbance change at 405 nm was recorded. All samples were performed in parallel.

The inhibition kinetic of compound **3q** against α-glucosidase was assayed with the same procedure abovementioned. For the inhibitory mechanism, the inhibitory activity of compound **3q** was assayed with different α-glucosidase concentration (Taha et al., 2017). For the inhibition type, the inhibitory activity of compound **3q** was assayed with different pNPG concentration (Khusnutdinova et al., 2017). The obtained curves revealed the kinetics of compound **3q**.

4.3. Fluorescence spectra

Fluorescence spectra of α-glucosidase with sample were recorded at 298, 304 and 310 K. Compound **3q** was titrimetrically added into α-glucosidase solution. The excitation wavelength was 280 nm and the emission wavelength was from 290 to 450 nm. The quenching mechanism was analyzed by Stern Volmer equation and the thermodynamic parameters were calculated using the Van't Hoff and the Gibbs-Helmholtz Eq (Jia et al., 2020; Jia et al., 2021).

4.4. 3D fluorescence spectra assay

To a PBS solution of α-glucosidase, compound **3q** was added, followed by the fluorescence spectra scanning at excitation and emission wavelengths of 200–600 nm and compared to that of α-glucosidase alone (Taha et al., 2016). The data is imported into Matlab for processing.

4.5. CD spectroscopy

To a solution of α-glucosidase, compound **3q** was added, followed by the CD spectrum scanning and compared to that of α-glucosidase alone (Taha et al., 2017). The CDNN was used to analyze the proportion of secondary conformation of protein.

4.6. Molecular docking

Molecular docking between compound **3q** and α-glucosidase was completed with SYBYL software using our previous method (Li et al., 2021). Compound **3q** was constructed, treated with energy minimization program, and charged with Gasteiger-Hückle model. The homology α-glucosidase protein was built according to previous works (Yu et al., 2018; Hu et al., 2021; Zhang et al., 2022), followed by the optimization of removing water molecules, adding hydrogen atoms, adding charge, and repairing end residues. After the active pocket was generated, the docking was operated. The protomol frid box dimensions data (x, y, z) was $27 \times 27 \times 25$. The results were visualized by Pymol and Discover studio software.

4.7. Statistical analysis

All data were presented as mean ± SD. One-way ANOVA was performed to evaluate the difference between groups. $P < 0.05$ was considered significant.

Declaration of Competing Interest

The authors declare that they have no known competing financial interests or personal relationships that could have appeared to influence the work reported in this paper.

Acknowledgements

This work was financially supported by the Fundamental and Applied Basic Research Fund of Guangdong Province (No. 2022A1515011657), Department of Education of Guangdong Province (Nos. 2019KZDXM035, 2021KTSCX135, 2021KCXTD044), and Jiangmen Science and Technology Plan Project (2021030103150006664). Special Funds for the Cultivation of Guangdong College Students' Scientific and Technological Innovation ("Climbing Program" Special Funds, pdjh2021a0504 and pdjh2022b0532).

References

Adeghate, E., Schattner, P., Dunn, E., 2006. An update on the etiology and epidemiology of diabetes mellitus. Ann. N. Y. Acad. Sci. 1084, 1–29.

Ali, F., Khan, K.M., Salar, U., Taha, M., Ismail, N.H., Wadood, A., Riaz, M., Perveen, S., 2017. Hydrazinyl arylthiazole based pyridine scaffolds: Synthesis, structural characterization, in vitro alpha-glucosidase inhibitory activity, and in silico studies. Eur. J. Med. Chem. 138, 255–272.

Catteau, L., Zhu, L., Van Bambeke, F., Quetin-Leclercq, J., 2018. Natural and hemi-synthetic pentacyclic triterpenes as antimicrobials and resistance modifying agents against Staphylococcus aureus: a review. Phytochem. Rev. 17 (5), 1129–1163.

DeFronzo, R.A., Ferrannini, E., Groop, L., Henry, R.R., Herman, W. H., Holst, J.J., Hu, F.B., Kahn, C.R., Raz, I., Shulman, G.I., Simonson, D.C., Testa, M.A., Weiss, R., 2015. Type 2 diabetes mellitus. Nat. Rev. Dis. Primers 1, 15019.

Deng, X.Y., Ke, J.J., Zheng, Y.Y., Li, D.L., Zhang, K., Zheng, X., Wu, J.Y., Xiong, Z., Wu, P.P., Xu, X.T., 2022. Synthesis and bioactivities evaluation of oleanolic acid oxime ester derivatives as alpha-glucosidase and alpha-amylase inhibitors. J. Enzyme Inhib. Med. Chem. 37 (1), 451–461.

Dhameja, M., Gupta, P., 2019. Synthetic heterocyclic candidates as promising alpha-glucosidase inhibitors: An overview. Eur. J. Med. Chem. 176, 343–377.

Ding, H., Wu, X., Pan, J., Hu, X., Gong, D., Zhang, G., 2018. New Insights into the Inhibition Mechanism of Betulinic Acid on alpha-Glucosidase. J. Agric. Food Chem. 66 (27), 7065–7075.

Ghani, U., 2015. Re-exploring promising alpha-glucosidase inhibitors for potential development into oral anti-diabetic drugs: Finding needle in the haystack. Eur. J. Med. Chem. 103, 133–162.

Guariguata, L., Whiting, D.R., Hambleton, I., Beagley, J., Linnenkamp, U., Shaw, J.E., 2014. Global estimates of diabetes prevalence for 2013 and projections for 2035. Diabetes Res. Clin. Pract. 103 (2), 137–149.

Hameed, S., Kanwal, F., Seraj, R., Rafique, S., Chigurupati, A., Wadood, A.U., Rehman, V., Venugopal, U., Salar, M., Taha, K. M.K., 2019. Synthesis of benzotriazoles derivatives and their dual potential as alpha-amylase and alpha-glucosidase inhibitors in vitro: Structure-activity relationship, molecular docking, and kinetic studies. Eur. J. Med. Chem. 183, 111677.

Hu, C.M., Wang, W.J., Ye, Y.N., Kang, Y., Lin, J., Wu, P.P., Li, D. L., Bai, L.P., Xu, X.T., Li, B.Q., Zhang, K., 2021. Novel cinnamic acid magnolol derivatives as potent alpha-glucosidase and alpha-amylase inhibitors: Synthesis, in vitro and in silico studies. Bioorg. Chem. 116, 105291.

Jia, Y., Gao, X., Xue, Z., Wang, Y., Lu, Y., Zhang, M., Panichayupakaranant, P., Chen, H., 2020. Characterization, antioxidant activities, and inhibition on α-glucosidase activity of corn silk polysaccharides obtained by different extraction methods. Int. J. Biol. Macromol. 163, 1640–1648.

Jia, Y., Xue, Z., Wang, Y., Lu, Y., Li, R., Li, N., Wang, Q., Zhang, M., Chen, H., 2021. Chemical structure and inhibition on α-glucosidase of polysaccharides from corn silk by fractional precipitation. Carbohyd. Polym. 252, 117185.

Kahn, S.E., Cooper, M.E., Del Prato, S., 2014. Pathophysiology and treatment of type 2 diabetes: perspectives on the past, present, and future. The Lancet 383 (9922), 1068–1083.

Kazakova, O.B., Giniyatullina, G.V., Mustafin, A.G., Babkov, D.A., Sokolova, E.V., Spasov, A.A., 2020. Evaluation of cytotoxicity and alpha-glucosidase inhibitory activity of amide and polyamino-derivatives of lupane triterpenoids. Molecules 25 (20).

Khusnutdinova, E.F., Smirnova, I.E., Kazakova, O.B., Petrova, A.V., Ha, N.T.T., Viet, D.Q., 2017. Synthesis and evaluation of 2,3-indolotriterpenoids as new α-glucosidase inhibitors. Med. Chem. Res. 26 (11), 2737–2742.

Khusnutdinova, E.F., Petrova, A.V., Thu, H.N.T., Tu, A.L.T., Thanh, T.N., Thi, C.B., Babkov, D.A., Kazakova, O.B., 2019. Structural modifications of 2,3-indolobetulinic acid: Design and synthesis of highly potent alpha-glucosidase inhibitors. Bioorg. Chem. 88, 102957.

Kim, S.J., Quan, H.Y., Jeong, K.J., Kim, D.Y., Kim, G., Jo, H.K., Chung, S.H., 2014. Beneficial effect of betulinic acid on hyperglycemia via suppression of hepatic glucose production. J. Agric. Food Chem. 62 (2), 434–442.

Leong, S.W., Abas, F., Lam, K.W., Yusoff, K., 2018. In vitro and in silico evaluations of diarylpentanoid series as alpha-glucosidase inhibitor. Bioorg. Med. Chem. Lett. 28 (3), 302–309.

Li, S., Yin, L., Yi, J., Zhang, L.M., Yang, L., 2021. Insight into interaction mechanism between theaflavin-3-gallate and alpha-glucosidase using spectroscopy and molecular docking analysis. J. Food Biochem. 45 (1), e13550.

Narender, T., Madhur, G., Jaiswal, N., Agrawal, M., Maurya, C.K., Rahuja, N., Srivastava, A.K., Tamrakar, A.K., 2013. Synthesis of novel triterpene and N-allylated/N-alkylated niacin hybrids as alpha-glucosidase inhibitors. Eur. J. Med. Chem. 63, 162–169.

Putta, S., Sastry Yarla, N., Kumar Kilari, E., Surekha, C., Aliev, G., Basavaraju Divakara, M., Sridhar Santosh, M., Ramu, R., Zameer, F., Prasad, N., Chintala, R., 2016. Therapeutic potentials of triterpenes in diabetes and its associated complications. Curr. Top. Med. Chem. 16 (23), 2532–2542.

Rafique, R., Khan, K.M., Arshia, K., Chigurupati, S., Wadood, A., Rehman, A.U., Karunanidhi, A., Hameed, S., Taha, M., Al-Rashida, M., 2020. Synthesis of new indazole based dual inhibitors of alpha-glucosidase and alpha-amylase enzymes, their in vitro, in silico and kinetics studies. Bioorg. Chem. 94, 103195.

Ramirez-Espinosa, J.J., Rios, M.Y., Lopez-Martinez, S., Lopez-Vallejo, F., Medina-Franco, J.L., Paoli, P., Camici, G., Navarrete-Vazquez, G., Ortiz-Andrade, R., Estrada-Soto, S., 2011. Antidiabetic activity of some pentacyclic acid triterpenoids, role of PTP-1B: in vitro, in silico, and in vivo approaches. Eur. J. Med. Chem. 46 (6), 2243–2251.

Saeedi, M., HadJiakhondi, A., Mohammad Nabavi, S., Manayi, A., 2017. Heterocyclic compounds: effective alpha-amylase and alpha-glucosidase inhibitors. Curr. Top. Med. Chem. 17, 428–440.

Taha, M., Ismail, N.H., Imran, S., Mohamad, M.H., Wadood, A., Rahim, F., Saad, S.M., Rehman, A.U., Khan, K.M., 2016. Synthesis, alpha-glucosidase inhibitory, cytotoxicity and docking studies of 2-aryl-7-methylbenzimidazoles. Bioorg. Chem. 65, 100–109.

Taha, M., Tariq Javid, M., Imran, S., Selvaraj, M., Chigurupati, S., Ullah, H., Rahim, F., Khan, F., Islam Mohammad, J., Mohammed Khan, K., 2017. Synthesis and study of the alpha-amylase inhibitory potential of thiadiazole quinoline derivatives. Bioorg. Chem. 74, 179–186.

Taha, M., Imran, S., Ismail, N.H., Selvaraj, M., Rahim, F., Chigurupati, S., Ullah, H., Khan, F., Salar, U., Javid, M.T., Vijayabalan, S., Zaman, K., Khan, K.M., 2017. Biology-oriented drug synthesis (BIODS) of 2-(2-methyl-5-nitro-1H-imidazol-1-yl)ethyl aryl ether derivatives, in vitro alpha-amylase inhibitory activity and in silico studies. Bioorg. Chem. 74, 1–9.

Wang, J., Lv, X., Xu, J., Liu, X., Du, T., Sun, G., Chen, J., Shen, X., Wang, J., Hu, L., 2020. Design, synthesis and biological evaluation of vincamine derivatives as potential pancreatic beta-cells protective agents for the treatment of type 2 diabetes mellitus. Eur. J. Med. Chem. 188, 111976.

Wang, G., Wang, J., Xie, Z., Chen, M., Li, L., Peng, Y., Chen, S., Li, W., Deng, B., 2017. Discovery of 3,3-di(indolyl)indolin-2-one as a novel scaffold for alpha-glucosidase inhibitors: In silico studies and SAR predictions. Bioorg. Chem. 72, 228–233.

Wang, G., Peng, Z., Wang, J., Li, X., Li, J., 2017. Synthesis, in vitro evaluation and molecular docking studies of novel triazine-triazole derivatives as potential alpha-glucosidase inhibitors. Eur. J. Med. Chem. 125, 423–429.

Wang, G., Peng, Z., Gong, Z., Li, Y., 2018. Synthesis, biological evaluation, and docking studies of novel 5,6-diaryl-1,2,4-triazine thiazole derivatives as a new class of alpha-glucosidase inhibitors. Bioorg. Chem. 78, 195–200.

Xu, X.T., Deng, X.Y., Chen, J., Liang, Q.M., Zhang, K., Li, D.L., Wu, P.P., Zheng, X., Zhou, R.P., Jiang, Z.Y., Ma, A.J., Chen, W. H., Wang, S.H., 2020. Synthesis and biological evaluation of coumarin derivatives as alpha-glucosidase inhibitors. Eur. J. Med. Chem. 189, 112013.

Yang, J.C., Li, H., Wang, X.L., Zhang, C.Y., Feng, G., Peng, X., 2021. Inhibition mechanism of α-amylase/α-glucosidase by silibinin, its synergism with acarbose, and the effect of milk proteins. J. Agric. Food Chem. 69, 10515–10526.

Yang, J.C., Wang, X.L., Zhang, C.Y., Ma, L., Wei, T., Zhao, Y.J., Peng, X., 2021. Comparative study of inhibition mechanisms of structurally different flavonoid compounds on α-glucosidase and synergistic effect with acarbose. Food Chem. 347, 129056.

Yu, Q., Wang, F., Hu, X., Xing, G., Deng, R., Guo, J., Cheng, A., Wang, J., Hao, J., Zhao, D., Teng, M., Zhang, G., 2018. Comparison of two docking methods for peptide-protein interactions. J. Sci. Food Agric. 98 (10), 3722–3727.

Zawawi, N.K., Taha, M., Ahmat, N., Ismail, N.H., Wadood, A., Rahim, F., Rehman, A.U., 2015. Synthesis, in vitro evaluation and molecular docking studies of biscoumarin thiourea as a new inhibitor of alpha-glucosidases. Bioorg. Chem. 63, 36–44.

Zhang, B.W., Xing, Y., Wen, C., Yu, X.X., Sun, W.L., Xiu, Z.L., Dong, Y.S., 2017. Pentacyclic triterpenes as alpha-glucosidase and alpha-amylase inhibitors: Structure-activity relationships and the synergism with acarbose. Bioorg. Med. Chem. Lett. 27 (22), 5065–5070.

Zhang, X., Zheng, Y.Y., Hu, C.M., Wu, X.Z., Lin, J., Xiong, Z., Zhang, K., Xu, X.T., 2022. Synthesis and biological evaluation of coumarin derivatives containing oxime ester as a-glucosidase inhibitors. Arab. J. Chem. 15, 104072.

Zheng, P.F., Xiong, Z., Liao, C.Y., Zhang, X., Feng, M., Wu, X.Z., Lin, J., Lei, L.S., Zhang, Y.C., Wang, S.H., Xu, X.T., 2021. In vitro and in silico studies of bis (indol-3-yl) methane derivatives as potential alpha-glucosidase and alpha-amylase inhibitors. J. Enzyme Inhib. Med. Chem. 36 (1), 1938–1951.